Enhancing the Production of Hydroxyl Radicals by *Pleurotus eryngii* via Quinone Redox Cycling for Pollutant Removal[▽]

Víctor Gómez-Toribio,[1]† Ana B. García-Martín,[2] María J. Martínez,[1]
Ángel T. Martínez,[1] and Francisco Guillén[2]*

*Centro de Investigaciones Biológicas, Consejo Superior de Investigaciones Científicas, Ramiro de Maeztu 9, 28040 Madrid, Spain,[1]
and Departamento de Microbiología y Parasitología, Universidad de Alcalá, Ctra. Madrid-Barcelona Km. 33.600,
28871 Alcalá de Henares, Madrid, Spain[2]*

The induction of hydroxyl radical ($^{\bullet}OH$) production via quinone redox cycling in white-rot fungi was investigated to improve pollutant degradation. In particular, we examined the influence of 4-methoxybenzaldehyde (anisaldehyde), Mn^{2+}, and oxalate on *Pleurotus eryngii* $^{\bullet}OH$ generation. Our standard quinone redox cycling conditions combined mycelium from laccase-producing cultures with 2,6-dimethoxy-1,4-benzoquinone (DBQ) and Fe^{3+}-EDTA. The main reactions involved in $^{\bullet}OH$ production under these conditions have been shown to be (i) DBQ reduction to hydroquinone ($DBQH_2$) by cell-bound dehydrogenase activities; (ii) $DBQH_2$ oxidation to semiquinone ($DBQ^{\bullet-}$) by laccase; (iii) $DBQ^{\bullet-}$ autoxidation, catalyzed by Fe^{3+}-EDTA, producing superoxide ($O_2^{\bullet-}$) and Fe^{2+}-EDTA; (iv) $O_2^{\bullet-}$ dismutation, generating H_2O_2; and (v) the Fenton reaction. Compared to standard quinone redox cycling conditions, $^{\bullet}OH$ production was increased 1.2- and 3.0-fold by the presence of anisaldehyde and Mn^{2+}, respectively, and 3.1-fold by substituting Fe^{3+}-EDTA with Fe^{3+}-oxalate. A 6.3-fold increase was obtained by combining Mn^{2+} and Fe^{3+}-oxalate. These increases were due to enhanced production of H_2O_2 via anisaldehyde redox cycling and $O_2^{\bullet-}$ reduction by Mn^{2+}. They were also caused by the acceleration of the DBQ redox cycle as a consequence of $DBQH_2$ oxidation by both Fe^{3+}-oxalate and the Mn^{3+} generated during $O_2^{\bullet-}$ reduction. Finally, induction of $^{\bullet}OH$ production through quinone redox cycling enabled *P. eryngii* to oxidize phenol and the dye reactive black 5, obtaining a high correlation between the rates of $^{\bullet}OH$ production and pollutant oxidation.

The degradation of lignin and pollutants by white-rot fungi is an oxidative and rather nonspecific process based on the production of substrate free radicals (36). These radicals are produced by ligninolytic enzymes, including laccase and three kinds of peroxidases: lignin peroxidase, manganese peroxidase, and versatile peroxidase (VP) (23). The H_2O_2 required for peroxidase activities is provided by several oxidases, such as glyoxal oxidase and aryl-alcohol oxidase (AAO) (9, 18). This free-radical-based degradative mechanism leads to the production of a broad variety of oxidized compounds. Common lignin depolymerization products are aromatic aldehydes and acids, and quinones (34). In addition to their high extracellular oxidation potential, white-rot fungi show strong ability to reduce these lignin depolymerization products, using different intracellular and membrane-bound systems (4, 25, 39). Since reduced electron acceptors of oxidized compounds are donor substrates for the above-mentioned oxidative enzymes, the simultaneous actions of both systems lead to the establishment of redox cycles (35). Although the function of these redox cycles is not fully understood, they have been hypothesized to be related to further metabolism of lignin depolymerization

products that require reduction to be converted in substrates of the ligninolytic enzymes (34). A second function attributed to these redox cycles is the production of reactive oxygen species, i.e., superoxide anion radicals ($O_2^{\bullet-}$), H_2O_2, and hydroxyl radicals ($^{\bullet}OH$), where lignin depolymerization products and fungal metabolites act as electron carriers between intracellular reducing equivalents and extracellular oxygen. This function has been studied in *Pleurotus eryngii*, whose ligninolytic system is composed of laccase (26), VP (24), and AAO (9). Incubation of this fungus with different aromatic aldehydes has been shown to provide extracellular H_2O_2 on a constant basis, due to the establishment of a redox cycle catalyzed by an intracellular aryl-alcohol dehydrogenase (AAD) and the extracellular AAO (7, 10). The process was termed aromatic aldehyde redox cycling, and 4-methoxybenzaldehyde (anisaldehyde) serves as the main *Pleurotus* metabolite acting as a cycle electron carrier (13). A second cyclic system, involving a cell-bound quinone reductase activity (QR) and laccase, was found to produce $O_2^{\bullet-}$ and H_2O_2 during incubation of *P. eryngii* with different quinones (11). The process was described as the cell-bound divalent reduction of quinones (Q) by QR, followed by extracellular laccase oxidation of hydroquinones (QH_2) into semiquinones ($Q^{\bullet-}$), which autoxidized to some extent, producing $O_2^{\bullet-}$ ($Q^{\bullet-} + O_2 \leftrightarrows Q + O_2^{\bullet-}$). H_2O_2 was formed by $O_2^{\bullet-}$ dismutation ($O_2^{\bullet-} + HO_2^{\bullet} + H^+ \rightarrow O_2 + H_2O_2$). In an accompanying paper, we describe the extension of this $O_2^{\bullet-}$ and H_2O_2 generation mechanism to $^{\bullet}OH$ radical production by the addition of Fe^{3+}-EDTA to incubation mixtures of several white-rot fungi with different quinones (6). Among them, those derived from 4-hydroxyphenyl, guaiacyl, and syringyl lignin units

were used: 1,4-benzoquinone (BQ), 2-methoxy-1,4-benzoquinone (MBQ), and 2,6-dimethyl-1,4-benzoquinone (DBQ), respectively. Semiquinone autoxidation under these conditions was catalyzed by Fe^{3+}-EDTA instead of being a direct electron transfer to O_2. The intermediate Fe^{2+}-EDTA reduced not only O_2, but also H_2O_2, leading to ·OH radical production by the Fenton reaction ($H_2O_2 + Fe^{2+} \rightarrow$ ·OH $+ OH^- + Fe^{3+}$).

Although ·OH radicals are the strongest oxidants produced by white-rot fungi (2, 14), studies of their involvement in pollutant degradation are quite scarce. In this context, the objectives of this study were to (i) determine possible factors enhancing the production of ·OH radicals by *P. eryngii* via quinone redox cycling and (ii) test the validity of this inducible ·OH production mechanism as a strategy for pollutant degradation. Our selection of possible ·OH production promoters was guided by two observations (6). First, the redox cycle of benzoquinones working with washed *P. eryngii* mycelium is rate limited by hydroquinone oxidation, since the amounts of the ligninolytic enzymes that remained bound to the fungus under these conditions were not large. Second, H_2O_2 is the limiting reagent for ·OH production by the Fenton reaction.

With these considerations in mind, anisaldehyde and Mn^{2+} were selected to increase H_2O_2 production. As mentioned above, anisaldehyde induces H_2O_2 production in *P. eryngii* via aromatic aldehyde redox cycling (7). Mn^{2+} has been shown to enhance H_2O_2 production during the oxidation of QH_2 by *P. eryngii* laccase by reducing the $O_2^{·-}$ produced in the semiquinone autoxidation reaction ($Mn^{2+} + O_2^{·-} \rightarrow Mn^{3+} + H_2O_2 + 2 H^+$) (26). Mn^{2+} was also selected to increase the hydroquinone oxidation rate, since this reaction has been shown to be propagated by the Mn^{3+} generated in the latter reaction ($QH_2 + Mn^{3+} \rightarrow Q^{·-} + Mn^{2+} + 2 H^+$). The replacement of Fe^{3+}-EDTA by Fe^{3+}-oxalate was also planned in order to increase the QH_2 oxidation rate above that resulting from the action of laccase. Oxalate is a common extracellular metabolite of wood-rotting fungi to which the function of chelating iron and manganese has been attributed (16, 45). The use of Fe^{3+}-oxalate and nonchelated Fe^{3+}, both QH_2 oxidants, has been proven to enable quinone redox cycling in fungi that do not produce ligninolytic enzymes, such as the brown-rot fungus *Gloeophyllum trabeum* (17, 40, 41). Finally, phenol and the azo dye reactive black 5 (RB5) were selected as model pollutants.

MATERIALS AND METHODS

Chemicals and enzymes. H_2O_2 (Perhydrol 30%) was obtained from Merck. 2-Deoxyribose, 2-thiobarbituric acid, bovine liver catalase, and oxalate oxidase were purchased from Sigma. 2,6-Dimethoxyphenol, 3,4-dimethoxybenzyl (veratryl) alcohol, 3,4,5-trimethoxybenzyl alcohol, 3,4,5-trimethoxybenzaldehyde, anisaldehyde, BQ, DBQ, 1,4-benzohydroquinone (BQH_2), 2-methoxy-BQH_2, hydroxybenzene (phenol), and 1,2-dihydroxybenzene (catechol) were from Aldrich. RB5 and 1,3-dihydroxybenzene (resorcinol) were from Sigma-Aldrich. 2,6-Dimethoxy-1,4-benzohydroquinone ($DBQH_2$) and MBQ were synthesized as previously reported (6). All other chemicals used were of analytical grade. Laccase isoenzyme I (EC 1.10.3.2) from *P. eryngii* was produced and purified as described previously (26).

Organism and culture conditions. *P. eryngii* IJFM A169 (Fungal Culture Collection of the Centro de Investigaciones Biológicas) (= ATCC 90787 and CBS 613.91) was grown in a glucose-peptone medium supplemented with 50 μM $MnSO_4$ in order to repress VP synthesis by the fungus (6). Oxalate production by the fungus was also investigated in the absence of Mn.

Enzyme activities. Washed mycelium was used for the determination of cell-bound laccase, AAO, QR, and AAD activities. Laccase and QR activities were estimated as reported in an accompanying paper (6). AAO activity was assayed in 100 mM phosphate buffer, pH 6, as the oxidation of veratryl alcohol to veratraldehyde (extinction coefficient at 310 nm [ε_{310}] = 9,300 M^{-1} cm^{-1}). For the determination of AAD activity, the substrate selected was 3,4,5-trimethoxybenzaldehyde to avoid, as much as possible, underestimations due to the action of AAO on its reduction product (3,4,5-trimethoxybenzyl alcohol). AAO activity on this alcohol has been shown to be quite low (9). QR activity was determined in 50 mM phosphate buffer, pH 5, containing 500 μM 3,4,5-trimethoxybenzaldehyde, as the production of 3,4,5-trimethoxybenzyl alcohol, which was analyzed by high-performance liquid chromatography (HPLC). Samples (20 μl) were injected into a Pharmacia system equipped with a Spherisorb S50DS2 column (Hichrom) and a diode array detector. The analyses were carried out at 40°C with a flow rate of 1 ml min^{-1} using 10 mM phosphoric acid-methanol (60/40) as the eluent. The alcohol concentrations in samples were calculated using a standard calibration curve. For these cell-bound analyses of enzymatic activities, appropriate amounts of mycelium were incubated at room temperature (22 to 25°C) with 20 ml substrate solutions in shaken 100-ml conical flasks (150 rpm). Samples were taken at 1-min intervals for 5 min. The mycelium was separated from the liquid by filtration. Absorbance was measured immediately after filtration for the analysis of laccase and AAO activities. The pH of samples used for the determination of QR and AAD activities was lowered to 2 with phosphoric acid, and they were kept frozen at −20°C until they were analyzed. International units (μmol min^{-1}) were used.

Redox cycling experiments. Anisaldehyde, BQ, MBQ, and DBQ (500 μM) redox cycling experiments were performed using 10-day-old pellets (202 ± 14 mg [dry weight]) as described previously (6). For ·OH production experiments, the complex 100 μM Fe^{3+}–110 μM EDTA and 2.8 mM 2-deoxyribose were added to the incubation mixture. Iron salt ($FeCl_3$) solutions were made up fresh immediately before use. Incubations were performed in the dark at 28°C and 150 rpm in 100-ml conical flasks. In phenol and RB5 degradation studies, initial concentrations of 500 and 50 μM were used, respectively. Samples were taken periodically from three replicate flasks, and the incubation liquid was separated from the mycelium by filtration. In order to inactivate laccase and AAO that could be released to the extracellular solution during the experiments, samples were treated in different ways depending on the kind of analysis to be done. For the analysis of quinone, hydroquinone, 2-thiobarbituric acid-reactive substances (TBARS), and phenol, the pH of samples was lowered to 2 with phosphoric acid. For H_2O_2 estimation, samples were heated at 80°C for 20 min (a treatment that does not affect H_2O_2 levels). The rest of the analyses were performed just after samples were taken. Verification of laccase and AAO inactivation by these treatments was carried out using a 10-day-old culture liquid sample.

Analytical techniques. The Somogyi-Nelson method for the determination of reducing sugars was used to estimate the glucose concentrations in fungal cultures (38).

Levels of DBQ, $DBQH_2$, phenol, catechol, resorcinol, and BQH_2 were determined by HPLC, using standard calibration curves for each compound and the same chromatographic conditions described above for AAD activity determination, except for the ratio of the phosphoric acid-methanol used as the eluent (80/20). The compounds were identified by comparing the retention time and spectrum with those of standards. Chemical and enzymatic oxidation of $DBQH_2$ was determined spectrophotometrically as DBQ production (ε_{397} = 562 M^{-1} cm^{-1}) (12). Oxalate production by *P. eryngii* was determined by HPLC, using oxalate oxidase to confirm the acid identity, as reported by Kuan and Tien (22).

H_2O_2 levels were estimated by measuring the production of O_2 with a Clark-type electrode after the addition of catalase to samples (6). The production of ·OH radicals was estimated as the conversion of 2-deoxyribose into TBARS (6). The RB5 concentration was determined spectrophotometrically at 596 nm. The molar extinction coefficient used was calculated using solutions of the dye in 20 mM phosphate buffer, pH 5, and proved to be 43,974 M^{-1} cm^{-1}.

Statistical analysis. All the results included in the text and shown in the figures are the means and standard deviations of three replicates (full biological experiments and technical analyses).

RESULTS

Selection of incubation conditions for quinone and aromatic aldehyde redox cycling. To study the effects of anisaldehyde, Mn^{2+}, and oxalate on the production of extracellular ·OH by *P. eryngii*, quinone redox cycling standard conditions were defined as follows: incubation of 10-day-old washed mycelium, grown under conditions expressing laccase as the sole ligninolytic enzyme, with a benzoquinone (usually DBQ) and Fe^{3+}-EDTA.
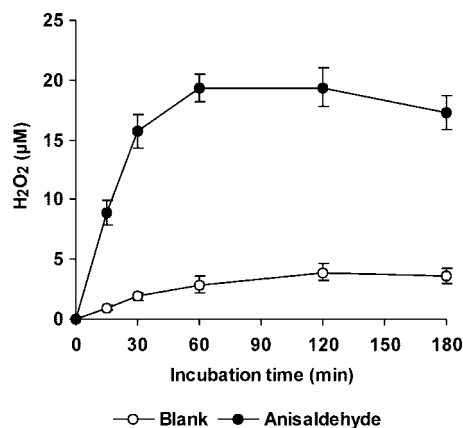
FIG. 1. Production of H_2O_2 by *P. eryngii* via anisaldehyde redox cycling. Ten-day-old washed mycelium was incubated with 1 mM anisaldehyde in 50 ml 20 mM phosphate buffer, pH 5. Anisaldehyde was omitted in blank incubations. The error bars indicate standard deviations.

FIG. 2. Effect of anisaldehyde on ·OH production by *P. eryngii* through the redox cycling of several benzoquinones. TBARS levels produced after 120-min incubation of the fungus with 500 μM BQ, MBQ, DBQ, or no quinone (No Q); 1 mM anisaldehyde; 100 μM Fe^{3+}–110 μM EDTA; and 2.8 mM 2-deoxyribose are shown. Anisaldehyde was absent in incubation blanks. The error bars indicate standard deviations.

Washed mycelium was used for two reasons: (i) to prevent, as much as possible, the reaction of ·OH radicals with compounds other than the probe used for their detection and (ii) to decrease the amount of laccase and thus to be able to evaluate better the effects of factors increasing hydroquinone oxidation. VP production was repressed to avoid (i) the consumption of the H_2O_2 required for ·OH production (6); (ii) the oxidation of Mn^{2+} (24), which could mask this reaction during the course of quinone redox cycling; and (iii) the oxidation of RB5 (15), which would hinder any effort made to ascribe a role to ·OH radicals in the degradation of the dye. Enzyme activity analysis in this mycelium showed that all the enzymes required for the catalysis of the redox cycling of quinones (QR and laccase) and aromatic aldehydes (AAD and AAO) were present. The amounts of the extracellular enzymes laccase and AAO that remained associated with the mycelium after being washed were 10.8 ± 1.5 and 7.3 ± 0.3 mU mg^{-1} (dry weight), respectively. The activities of intracellular dehydrogenases were shown to be 27.8 ± 3.1 and 1.2 ± 0.1 mU mg^{-1} for QR and AAD, respectively.

Effect of anisaldehyde on ·OH production. The time course of production of extracellular H_2O_2 by washed *P. eryngii* mycelium when incubated with anisaldehyde is shown in Fig. 1. Constant H_2O_2 levels reached after 60 min of incubation increased from 3.5 to 18.6 μM (average of 60- to 180-min samples). This increase was caused by the concerted actions of AAD reducing anisaldehyde and AAO oxidizing anisyl alcohol. In order to test if this increase had any effect on ·OH production by the fungus, anisaldehyde was included in quinone redox cycling experiments carried out with BQ, MBQ, and DBQ. In all cases, the presence of anisaldehyde enhanced ·OH production, which was linear during the 180 min that the experiments lasted (data not shown). Figure 2 shows TBARS levels in 120-min samples. Regardless of anisaldehyde inclusion, the highest values were found in incubations with DBQ, followed by MBQ, BQ, and no Q. In quantitative terms, the increase caused by anisaldehyde followed the opposite order: 2.0-, 1.9-, 1.5-, and 1.2-fold higher in incubations with no Q, BQ, MBQ, and DBQ, respectively. H_2O_2 production in these incubations without anisaldehyde has been reported to reach
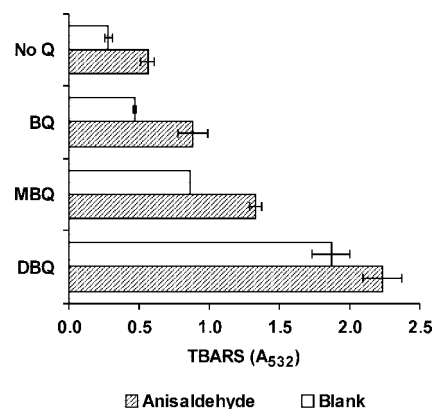
constant 4, 8, 72, and 192 μM levels with no Q, BQ, MBQ, and DBQ, respectively (6). Therefore, the lower these levels, the greater the effect of anisaldehyde on ·OH radical production.

Effect of Mn^{2+} on ·OH production. DBQ was selected for experiments evaluating the effect of Mn^{2+} on ·OH production by *P. eryngii*. The two effects expected to be caused by Mn^{2+} on quinone redox cycling (increased H_2O_2 production by reduction of $O_2^{·-}$ and propagation of $DBQH_2$ oxidation by the resulting Mn^{3+}) were first evaluated in vitro. The reactions were carried out in 20 mM phosphate buffer, pH 5, with purified laccase I from *P. eryngii* and $DBQH_2$. H_2O_2 levels, estimated after full oxidation of 100 μM $DBQH_2$ in the absence and presence of 100 μM Mn^{2+}, were found to be 9.0 ± 0.3 and 50.2 ± 0.7 μM, respectively. The oxidation rate of $DBQH_2$ (500 μM) increased from 37 ± 1 μM min^{-1} in reactions without Mn^{2+} to 296 ± 4 μM min^{-1} in reactions containing 100 μM Mn^{2+}. These two Mn effects were then tested in vivo during the incubation of *P. eryngii* with DBQ in the absence of Fe^{3+}-EDTA. The levels of H_2O_2, DBQ, and $DBQH_2$ at system equilibrium in the absence and presence of different Mn^{2+} concentrations are shown in Fig. 3. Mn^{2+} exerted a pronounced effect on the three parameters being analyzed. H_2O_2 levels increased as the Mn^{2+} concentration did, with no significant differences observed beyond 100 μM. The presence of Mn^{2+} also decreased $DBQH_2$/DBQ ratios in samples, showing the propagation of $DBQH_2$ oxidation by Mn^{3+} and, therefore, the acceleration of the DBQ redox cycle. The global effect of Mn^{2+} on ·OH production was evaluated in parallel incubations with DBQ including Fe^{3+}-EDTA (Fig. 4). The TBARS production rate improved from 12 mU A_{532} min^{-1} (incubation without Mn^{2+}) to 19 and 36 mU A_{532} min^{-1} in incubations with 20 and 100 μM Mn^{2+}, respectively. Similarly to the H_2O_2 production levels depicted in Fig. 3, a further increase of the Mn^{2+} concentration to 250 and 500 μM did not lead to any significant increase in the TBARS production rate.

Effect of oxalate on ·OH production and phenol oxidation. The capability of *P. eryngii* to produce oxalate is shown in Fig. 5. Oxalate was detected only when the fungus was grown in the
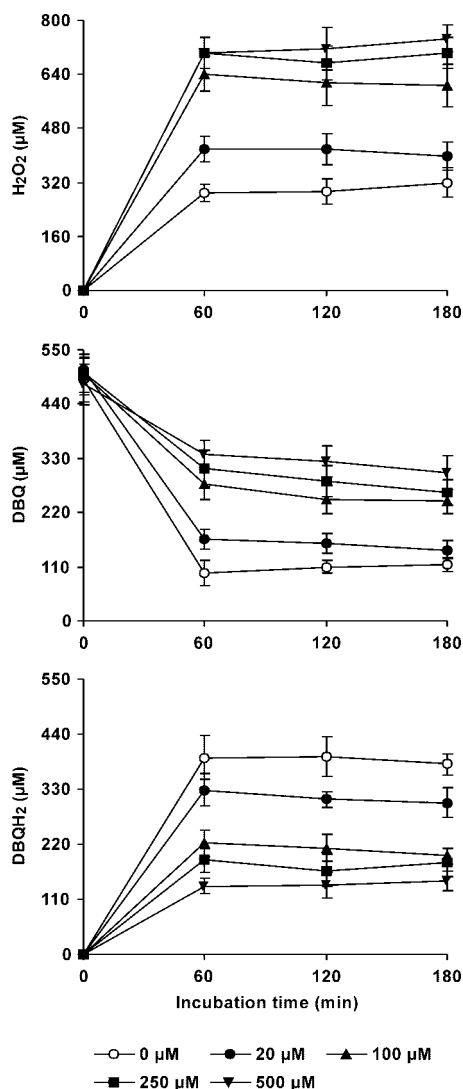
FIG. 3. Effects of different concentrations of Mn^{2+} on H_2O_2 production and $DBQ(H_2)$ levels during the incubation of *P. eryngii* with DBQ. Washed mycelium was incubated with 500 μM DBQ in the absence and presence of 20, 100, 250, and 500 μM Mn^{2+}. The error bars indicate standard deviations.

FIG. 4. Effects of different concentrations of Mn^{2+} on ·OH production by *P. eryngii* via DBQ redox cycling. The incubation mixtures were as described in the legend to Fig. 3 plus 100 μM Fe^{3+}–110 μM EDTA and 2.8 mM 2-deoxyribose. The error bars indicate standard deviations.

vitro to be caused by Fe^{3+}-oxalate in the $DBQH_2$ oxidation rate. As a consequence, the TBARS production rate was about threefold greater with Fe^{3+}-oxalate than with Fe^{3+}-EDTA. TBARS production in the absence of DBQ was also observed in both cases, although at a much lower rate and showing no significant differences between them. We have previously reported that Fe^{3+}-EDTA reduction by an unknown cell-bound system was causing ·OH production in incubation blanks without quinones (6). The TBARS production rate (Fig. 6) was shown to be constant with Fe^{3+}-EDTA during the whole period of study (14.4 mU A_{532} min^{-1}). However, with Fe^{3+}-oxalate, it decreased gradually from 39.0 mU A_{532} min^{-1} during the first hour to 31.4 and 19.5 mU A_{532} min^{-1} during the second and third hours, respectively. Among the possible causes, DBQ consumption was clearly observed. Thus, whereas the sum of the DBQ and $DBQH_2$ levels in samples from Fe^{3+}-EDTA incubations remained steady around 468 μM (average of 30- to 180-min samples), in the case of Fe^{3+}-oxalate, decreases from the initial 500 μM DBQ concentration to 386

absence of Mn^{2+}. The highest levels (around 2.8 mM) were measured after 10 days, when glucose had been nearly depleted (6). The effect of replacing Fe^{3+}-EDTA by Fe^{3+}-oxalate on ·OH production was also studied during the DBQ redox cycle. Since the aim of this replacement was to increase the $DBQH_2$ oxidation rate, the likelihood of Fe^{3+}-oxalate acting as a $DBQH_2$ oxidant was first tested. Compared with 100 μM Fe^{3+}–110 μM EDTA, which prevented the oxidation of 500 μM $DBQH_2$ (5-min reactions in 20 mM phosphate buffer, pH 5), 100 μM Fe^{3+}–500 μM oxalate oxidized $DBQH_2$ at a rate of 20.6 $\pm$ 0.3 μM min^{-1}. Figure 6A and B shows the effect caused by Fe^{3+}-oxalate on the DBQ redox cycle and TBARS production, respectively. The replacement of Fe^{3+}-EDTA by Fe^{3+}-oxalate produced a decrease in the $DBQH_2$/DBQ concentration ratio in all samples. These results indicated that the redox cycle rate was raised, according to the increase seen in
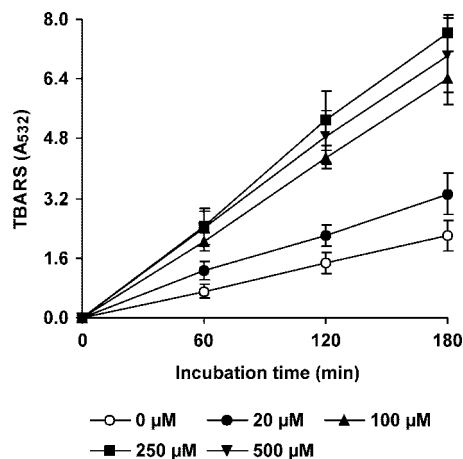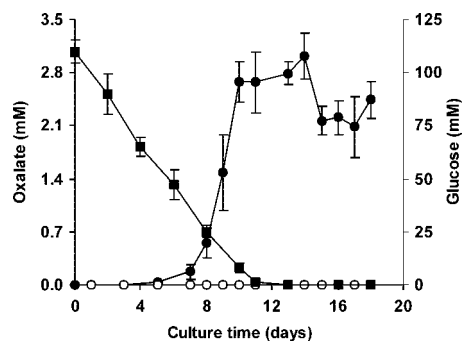

FIG. 5. Time course of oxalate production (●) and glucose consumption (■) by *P. eryngii* in glucose-peptone medium. Cultures were carried out in the absence (filled symbols) and presence (open symbols) of 50 μM $MnSO_4$. Glucose levels without Mn were not significantly different from those with Mn (data not shown). The error bars indicate standard deviations.
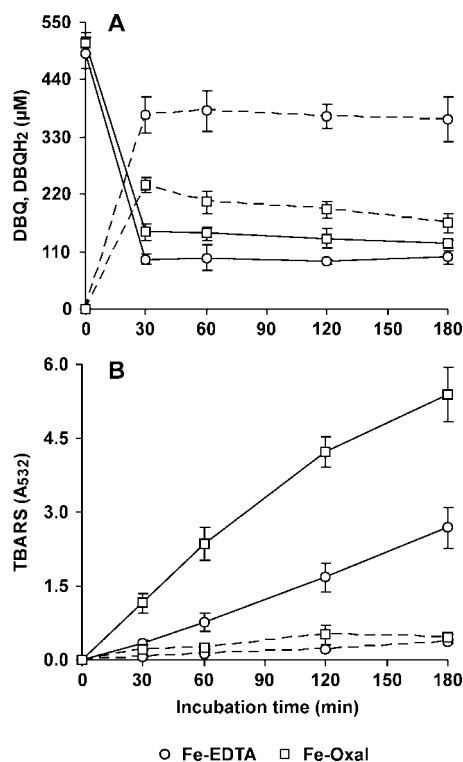
○ Fe-EDTA   □ Fe-Oxal

FIG. 6. Effects of oxalate, used as an iron-chelating agent, on DBQ(H$_2$) levels and ˙OH production during the incubation of *P. eryngii* with DBQ. The incubation mixtures contained 500 μM DBQ, 2.8 mM 2-deoxyribose, and either 100 μM Fe^{3+}–110 μM EDTA or 100 μM Fe^{3+}–500 μM oxalate. (A) DBQ (solid lines) and DBQH$_2$ (dashed lines) levels. (B) TBARS levels in whole incubations (solid lines) and blanks without DBQ (dashed lines). The error bars indicate standard deviations.

μM in the 30-min sample and 290 μM in the 180-min sample were found. Afterward, ˙OH production was optimized in terms of both the Fe^{3+}/oxalate ratio and the concentration of the best ratio obtained. Figure 7 shows an optimal Fe^{3+}/oxalate ratio of 1:3, although no significant differences in the TBARS production rates were observed from the 1:2 to 1:5
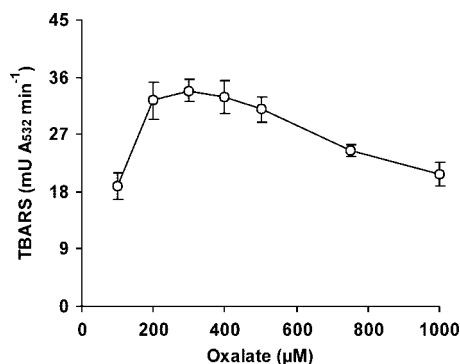

FIG. 7. Effect of the Fe^{3+}/oxalate concentration ratio on ˙OH production by *P. eryngii* via DBQ redox cycling. Washed mycelium was incubated with 500 μM DBQ, 2.8 mM 2-deoxyribose, and 100 μM Fe^{3+} chelated with different oxalate concentrations. The error bars indicate standard deviations.
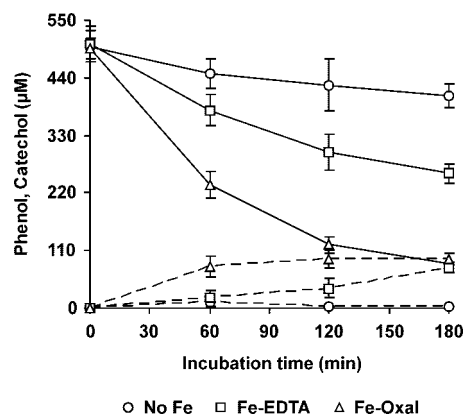

○ No Fe   □ Fe-EDTA   △ Fe-Oxal

FIG. 8. Phenol removal by *P. eryngii* under conditions producing different levels of ˙OH radicals. Incubations of washed mycelium with 500 μM concentrations of phenol and DBQ were performed in the absence (no Fe) and presence of 100 μM Fe^{3+}–110 μM EDTA or 100 μM Fe^{3+}–300 μM oxalate. The time courses of phenol disappearance and catechol production are shown (solid and dashed lines, respectively). The error bars indicate standard deviations.

ratios. Using the 1:3 Fe^{3+}/oxalate ratio, no significant differences were observed in the TBARS production rates using concentrations ranging from 100:300 to 1,000:3,000 μM (data not shown).

To better ascribe a role to ˙OH radicals in the oxidation of pollutants, two DBQ redox cycling incubation conditions leading to quite different TBARS production rates were used. Thus, phenol oxidation was studied using Fe^{3+}-EDTA and Fe^{3+}-oxalate complexes. Phenol removal was clearly associated with induction of ˙OH radical production (Fig. 8). We have previously reported that phenol is not a substrate of *P. eryngii* laccase (27). Due to phenol volatility, a gradual decrease in its initial concentration was observed in the different incubation controls used. After subtracting this decrease, the extents of phenol removal in 180-min samples in incubations with Fe^{3+}-EDTA and Fe^{3+}-oxalate were 29 and 64%, respectively. As hydroxylation is one of the main reactions caused by ˙OH radicals when acting on aromatic compounds, samples were analyzed for the production of the three possible dihydroxylated phenol derivatives, i.e., catechol, resorcinol and BQH$_2$. Among them, only catechol was detected in all samples (Fig. 8). BQH$_2$ was sporadically found in some samples (6.2 μM was the highest level detected), and resorcinol was always absent (data not shown).

Combined effects of oxalic acid and Mn^{2+} on ˙OH production and RB5 oxidation. A combination of Fe^{3+}-oxalate and Mn^{2+} to promote ˙OH radical production was included in RB5 degradation studies. Figure 9 shows the effect of Mn^{2+} on TBARS production by *P. eryngii* in incubations with DBQ and Fe^{3+}-oxalate. The TBARS production rate, calculated from the results obtained during the first 60 min, increased from 43.6 to 91.1 mU A_{532} min^{-1} by the addition of Mn^{2+}. This represents a 6.3-fold increase relative to the rate observed in incubations with Fe^{3+}-EDTA (Fig. 6B). RB5 oxidation results obtained under the same ˙OH radical induction conditions are shown in Fig. 10. The dye was oxidized only when ˙OH radicals were produced, showing a high correlation with the TBARS produced under each incubation condition (Fig. 9). Thus, the
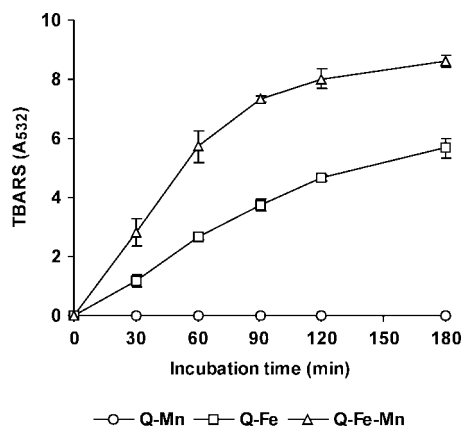
FIG. 9. Effect of Mn^{2+} on ·OH production by *P. eryngii* in incubations with DBQ and Fe^{3+}-oxalate. The incubation mixtures contained 500 μM DBQ, 100 μM Fe^{3+}–300 μM oxalate, 2.8 mM 2-deoxyribose, and 100 μM Mn^{2+} (Q-Fe-Mn). Incubation blanks without Mn (Q-Fe) or Fe^{3+}-oxalate (Q-Mn) were performed. The error bars indicate standard deviations.

FIG. 10. RB5 removal by *P. eryngii* under conditions producing different levels of ·OH radicals. The composition of the reaction mixtures was as described in the legend to Fig. 9, except 2-deoxyribose was replaced by 50 μM RB5. The error bars indicate standard deviations.

extents of degradation observed after 3 h were 68 and 85% in the absence and presence of Mn^{2+}, respectively. Incubation blanks in these experiments were carried out with DBQ and Mn^{2+}, but in the absence of Fe^{3+}-oxalate, as the Mn^{3+} produced in the course of the DBQ redox cycle could oxidize RB5. Figure 10 shows that this was not the case. The lack of laccase activity on RB5 was confirmed in in vitro reactions with purified enzyme.

DISCUSSION

The production of ·OH radicals by *P. eryngii* via DBQ redox cycling in the presence of Fe^{3+}-EDTA is illustrated in Fig. 11 by reactions 1 to 5. In the accompanying paper (6), we reported that after DBQ reduction by QR (reaction 1) and $DBQH_2$ oxidation by laccase (reaction 2), the production of $O_2^{·-}$ by $DBQ^{·-}$ autoxidation (reaction 3) is mainly catalyzed by Fe^{3+}-EDTA (reactions 3a and 3b). Fenton's reagent formation is accomplished by $O_2^{·-}$ dismutation (reaction 4), and as a result, ·OH radicals are generated (reaction 5). In the present study, we have identified three approaches to increase ·OH production by this mechanism. Two are based on the enhancement exerted by adequate metal ions on the $DBQH_2$ oxidation rate and H_2O_2 production during the course of quinone redox cycling. The third approach implies the induction of aromatic aldehyde redox cycling, which increases H_2O_2 production further to that caused by quinone redox cycling itself.

The addition of Mn^{2+} to DBQ redox cycling experiments was shown to increase H_2O_2 levels and the $DBQH_2$ oxidation rate (Fig. 3), improving ·OH radical production (Fig. 4). The reactions involving Mn^{2+}, shown in Fig. 11, are the reduction of $O_2^{·-}$ to H_2O_2 (reaction 6) and the oxidation of $DBQH_2$ by the resulting Mn^{3+} (reaction 7). Stoichiometrically, the first reaction doubles the amount of H_2O_2 produced by $O_2^{·-}$ dismutation. Since $DBQ^{·-}$ autoxidation is a reversible reaction, the consumption of $O_2^{·-}$ by Mn^{2+} shifts equilibrium toward the right, favoring this reaction over other competing reactions converting $DBQ^{·-}$ into DBQ (dismutation and oxidation by
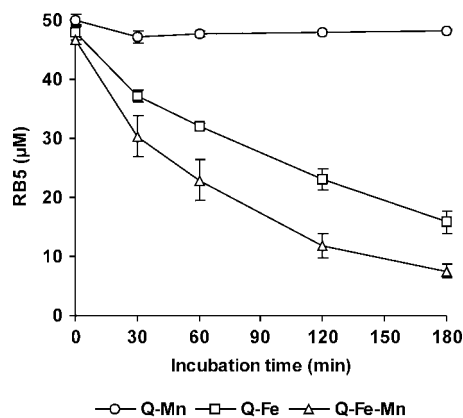
laccase) (12). The results supporting the propagation of $DBQH_2$ oxidation by Mn^{3+} were as follows: (i) the decrease in the $DBQH_2$/DBQ ratios observed in redox cycling experiments carried out in the presence of different concentrations of Mn^{2+} (Fig. 3) and (ii) the eightfold increase caused by Mn^{2+} in the rate of $DBQH_2$ oxidation catalyzed by purified laccase (see above). We have previously reported that the addition of superoxide dismutase to laccase reaction mixtures with the same composition increased the rate of $DBQH_2$ oxidation by only 1.1 times (12) (superoxide dismutase shifts $DBQ^{·-}$ autoxidation reaction to DBQ production by consuming $O_2^{·-}$, as Mn^{2+} does, but has no effect on the hydroquinone oxidation rate). Demonstration of Mn^{3+} production through quinone redox cycling (a sequence of reactions 1 to 3 and 6 in Fig. 11) provides in vivo validation of our previous finding of the involvement of laccase in Mn^{2+} oxidation (11, 26, 33). Furthermore, it implies the cooperation of QR activities by the recycling of laccase reaction products. Therefore, we extend to quinone redox cycling our earlier proposal of hydroquinone oxidation by laccase as an alternative mechanism to manganese peroxidase- and VP-mediated production of Mn^{3+}.

A second successful strategy to improve ·OH production was the substitution of Fe^{3+}-EDTA by Fe^{3+}-oxalate (Fig. 6). The use of Fe^{3+}-EDTA, preventing hydroquinone oxidation by this metal ion, was shown to be a useful tool to ascribe a role to ligninolytic enzymes in quinone redox cycling (6). However, chemical oxidation of hydroquinones by Fe^{3+} complexes involving white-rot fungus metabolites, such as oxalate, could also play a role in the process, as reported in *G. trabeum* (40, 41). The capability of *P. eryngii* to produce oxalate is shown for the first time in the present study (Fig. 5). Further research is required in order to know if the absence of oxalate in cultures containing Mn^{2+} was due to repression of its synthesis or its continuous consumption. Although VP production is repressed in the presence of Mn^{2+} (6), the existence of an alternative mechanism providing Mn^{3+}, which has been shown to oxidize oxalate (22), cannot be excluded. The results shown in Fig. 6 demonstrated that the oxidation of $DBQH_2$ by Fe^{3+}-oxalate makes a good contribution to ·OH production. This reaction, labeled 8 in Fig. 11, leads to the production of Fe^{2+}-oxalate,
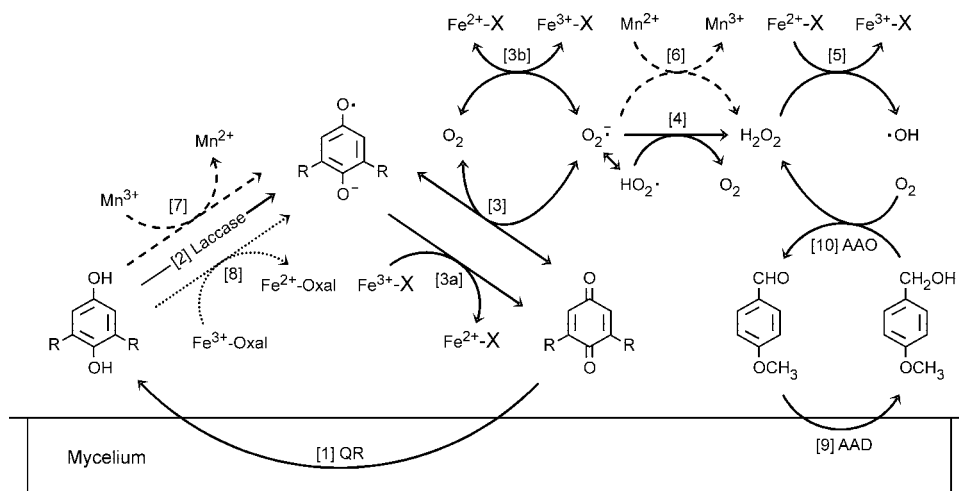
FIG. 11. Scheme showing the main reactions involved in the production of $^\bullet$OH radicals by *P. eryngii* via DBQ redox cycling in the presence of Mn^{2+}, the complex Fe^{3+}-oxalate, and anisaldehyde. $R = OCH_3$, and $X = EDTA$ or oxalate (see Discussion for an explanation).

whose involvement in the reduction of O_2 (reaction 3b) and H_2O_2 (reaction 5) has been previously reported (28). Compared with Fe^{3+}-EDTA, one distinctive effect of Fe^{3+}-oxalate on the DBQ redox cycle has been the progressive consumption of DBQ(H_2) (Fig. 6), which could be attributed to an increase in $^\bullet$OH production. It seems unlikely that other possible oxalate side reactions occurring during the course of quinone redox cycling could have a direct effect on DBQ(H_2) removal, although they may affect the rate of redox cycling. For instance, the production of the powerful reducing agent formate anion radical ($CO_2^{\bullet-}$) through the oxidation of oxalate by $^\bullet$OH ($^\bullet$OH + oxalate $\rightarrow CO_2^{\bullet-} + CO_2 + H_2O$) (3, 41) could increase $O_2^{\bullet-}$ production via autoxidation ($CO_2^{\bullet-} + O_2 \rightarrow CO_2 + O_2^{\bullet-}$) (31), as well as the reduction rates of iron (19) and most probably quinone. In terms of the TBARS production rate, the contribution of Fe^{3+}-oxalate (Fig. 6) was similar to that observed with Mn^{2+} (Fig. 4), i.e., a threefold increase. The combination of Fe^{3+}-oxalate and Mn^{2+} increased this parameter two more times (Fig. 9). In the presence of oxalate and Mn^{2+}, H_2O_2 production could be promoted, not only by the reduction of $O_2^{\bullet-}$ by Mn^{2+} (Fig. 11, reaction 6), but also by the production of $CO_2^{\bullet-}$ through the oxidation of oxalate by the resulting Mn^{3+} (oxalate + $Mn^{3+} \rightarrow CO_2^{\bullet-} + CO_2 + Mn^{2+}$), followed by $CO_2^{\bullet-}$ autoxidation and either $O_2^{\bullet-}$ dismutation or reduction by Mn^{2+} (22). Although the oxidation of oxalate by $^\bullet$OH and Mn^{2+} could have a positive effect on H_2O_2 production, the occurrence of these reactions would consume oxalate. This consumption, joined to the disappearance of DBQ(H_2) (Fig. 6), could explain the decline of the TBARS production rate observed after 60 min under these conditions (Fig. 9). It is also likely that this decline was caused by the uptake of iron by the fungus, which could be facilitated by its binding to oxalate (EDTA has been reported to inhibit this process [20]).

The third approach to improve $^\bullet$OH production by *P. eryngii* consisted of anisaldehyde addition to fungal incubations with ferric iron and different quinones. Our results show that this improvement is due to increased H_2O_2 production by the fungus via anisaldehyde redox cycling (Fig. 1 and 2). Reactions 9 and 10 in Fig. 11 illustrate this process. From the constant

H_2O_2 levels observed in incubations of *P. eryngii* with 1 mM anisaldehyde (19 μM) (Fig. 1) and those previously found in incubations with 500 μM BQ, MBQ, and DBQ (8, 72, and 192 μM, respectively) (6), it is noticeable that the redox cycling of methoxyquinones is a much more efficient H_2O_2 production mechanism than that of aromatic aldehydes. Thus, the increase caused by anisaldehyde in $^\bullet$OH production with these quinones, mainly with DBQ (1.2 times), was small (Fig. 2). This increase was nearly insignificant compared with that caused by Mn^{2+} or Fe^{3+}-oxalate in DBQ incubations (three times) (Fig. 4 and 6B, respectively). This led us to discard anisaldehyde as a factor promoting $^\bullet$OH production in pollutant removal studies. Regardless, the results shown in Fig. 2 are of interest, since they confirm the cooperation of laccase and AAO for $^\bullet$OH production (8), which we have shown incorporates QR and AAD activities. In other words, quinone and aromatic aldehyde redox cycling acting together for $^\bullet$OH production has been demonstrated.

Under the incubation conditions used in the present study (washed mycelium producing laccase as the sole ligninolytic enzyme), the induction of $^\bullet$OH production enabled *P. eryngii* to degrade the two pollutants tested. This has been shown by the high correlation between the rates of phenol and RB5 removal (Fig. 8 and 10, respectively) and those of TBARS production observed in each case (Fig. 6B and 9, respectively). These results support our previous proposal for the use of quinone redox cycling as a useful tool to increase $^\bullet$OH production in white-rot fungi and to enable us to ascribe a role to these radicals in pollutant degradation. In brown-rot fungi, whose degradative capability is mainly due to $^\bullet$OH radical production, quinone redox cycling studies have provided good evidence of the crucial role these radicals play in the degradation of polyethylene glycol by *G. trabeum* (17) and 2-fluorophenol by *Gloeophyllum striatum* (21). The results shown in Fig. 8 and 10 also provide the basis for the use of quinone redox cycling as a strategy to increase the degradative capability of white-rot fungi with regard to pollutants. Although the production of $^\bullet$OH radicals by white-rot fungi has not yet been taken advantage of for this purpose, physical-chemical processes based on

the formation of these radicals have gained great attention in recent years due to their high efficiency in the degradation and even mineralization of pollutants (29, 30, 44). These processes, some of them based on Fenton's reagent, are referred to as advanced oxidation processes (5). In the present study, catechol and BQH$_2$ have been identified as phenol degradation intermediates (Fig. 8). Degradation studies of phenolic compounds and azo dyes (including phenol and RB5) by different advanced oxidation processes have shown not only the production of hydroquinones as primary intermediates, but also of quinones and oxalate as consecutive intermediates (1, 37, 42, 43).

From these observations, two interesting inferences can be drawn. First, although mineralization of pollutants is possible by ·OH radical attack, their initial conversion into hydroquinones can facilitate the degradative process, as these intermediates are well-known substrates of the ligninolytic enzymes. For instance, the two hydroquinones derived from phenol hydroxylation (catechol and BQH$_2$) have been shown to be oxidized by *P. eryngii* laccase (26). Furthermore, catechol is susceptible to ring cleavage by intracellular dioxygenases already characterized in white-rot fungi (32). Second, although the quinone used to induce ·OH production, and probably oxalate, is consumed during quinone redox cycling (Fig. 6), the production of similar or the same pollutant degradation intermediates can sustain the production of ·OH radicals. In this respect, we have already shown that BQ and 2-methyl-1,4-naphthoquinone (menadione), which can derive from ·OH attack on phenol and 2-methylnaphthalene, respectively, support ·OH radical production (6). More work is needed to corroborate the notion that the induction of ·OH production in white-rot fungi via quinone redox cycling improves their degradative capabilities. In this regard, our research group is investigating the degradation of a wide range of recalcitrant and toxic compounds by several white-rot fungi using this strategy.

REFERENCES

1. **Alnaizy, R., and A. Akgerman.** 2000. Advanced oxidation of phenolic compounds. Adv. Environ. Res. **4:**233–244.
2. **Backa, S., J. Gierer, T. Reitberger, and T. Nilsson.** 1993. Hydroxyl radical activity associated with the growth of white-rot fungi. Holzforschung **47:**181–187.
3. **Cameron, M. D., and S. D. Aust.** 1999. Degradation of chemicals by reactive radicals produced by cellobiose dehydrogenase from *Phanerochaete chrysosporium*. Arch. Biochem. Biophys. **367:**115–121.
4. **Constam, D., A. Muheim, W. Zimmermann, and A. Fiechter.** 1991. Purification and partial characterization of an intracellular NADH:quinone oxidoreductase from *Phanerochaete chrysosporium*. J. Gen. Microbiol. **137:**2209–2214.
5. **Glaze, W. H., J. W. Kang, and D. H. Chapin.** 1987. The chemistry of water treatment processes involving ozone, hydrogen peroxide and ultraviolet radiation. Ozone Sci. Eng. **9:**335–352.
6. **Gómez-Toribio, V., A. B. García-Martín, M. J. Martínez, Á. T. Martínez, and F. Guillén.** 2009. Induction of extracellular hydroxyl radical production by white-rot fungi through quinone redox cycling. Appl. Environ. Microbiol. **75:**3944–3953.
7. **Guillén, F., and C. S. Evans.** 1994. Anisaldehyde and veratraldehyde acting as redox cycling agents for H$_2$O$_2$ production by *Pleurotus eryngii*. Appl. Environ. Microbiol. **60:**2811–2817.
8. **Guillén, F., V. Gómez-Toribio, M. J. Martínez, and A. T. Martínez.** 2000. Production of hydroxyl radical by the synergistic action of fungal laccase and aryl alcohol oxidase. Arch. Biochem. Biophys. **383:**142–147.
9. **Guillén, F., A. T. Martínez, and M. J. Martínez.** 1992. Substrate specificity and properties of the aryl-alcohol oxidase from the ligninolytic fungus *Pleurotus eryngii*. Eur. J. Biochem. **209:**603–611.
10. **Guillén, F., A. T. Martínez, M. J. Martínez, and C. S. Evans.** 1994. Hydrogen peroxide-producing system of *Pleurotus eryngii* involving the extracellular enzyme aryl-alcohol oxidase. Appl. Microbiol. Biotechnol. **41:**465–470.
11. **Guillén, F., M. J. Martínez, C. Muñoz, and A. T. Martínez.** 1997. Quinone redox cycling in the ligninolytic fungus *Pleurotus eryngii* leading to extracellular production of superoxide anion radical. Arch. Biochem. Biophys. **339:**190–199.
12. **Guillén, F., C. Muñoz, V. Gómez-Toribio, A. T. Martínez, and M. J. Martínez.** 2000. Oxygen activation during the oxidation of methoxyhydroquinones by laccase from *Pleurotus eryngii*. Appl. Environ. Microbiol. **66:**170–175.
13. **Gutiérrez, A., L. Caramelo, A. Prieto, M. J. Martínez, and A. T. Martínez.** 1994. Anisaldehyde production and aryl-alcohol oxidase and dehydrogenase activities in ligninolytic fungi from the genus *Pleurotus*. Appl. Environ. Microbiol. **60:**1783–1788.
14. **Hammel, K. E., A. N. Kapich, K. A. Jensen, and Z. C. Ryan.** 2002. Reactive oxygen species as agents of wood decay by fungi. Enzyme Microb. Technol. **30:**445–453.
15. **Heinfling, A., M. J. Martínez, A. T. Martínez, M. Bergbauer, and U. Szewzyk.** 1998. Transformation of industrial dyes by manganese peroxidase from *Bjerkandera adusta* and *Pleurotus eryngii* in a manganese-independent reaction. Appl. Environ. Microbiol. **64:**2788–2793.
16. **Henry, W. P.** 2003. Non-enzymatic iron, manganese, and copper chemistry of potential importance in wood decay, p. 175–195. *In* B. Goodell, D. D. Nicholas, and T. P. Schultz (ed.), Wood deterioration and preservation. Advances in our changing world. Oxford University Press, Washington, DC.
17. **Kerem, Z., K. A. Jensen, and K. E. Hammel.** 1999. Biodegradative mechanism of the brown rot basidiomycete *Gloeophyllum trabeum*: evidence for an extracellular hydroquinone-driven Fenton reaction. FEBS Lett. **446:**49–54.
18. **Kersten, P. J., and T. K. Kirk.** 1987. Involvement of a new enzyme, glyoxal oxidase, in extracellular H$_2$O$_2$ production by *Phanerochaete chrysosporium*. J. Bacteriol. **169:**2195–2201.
19. **Khindaria, A., T. A. Grover, and S. D. Aust.** 1994. Oxalate-dependent reductive activity of manganese peroxidase from *Phanerochaete chrysosporium*. Arch. Biochem. Biophys. **314:**301–306.
20. **Kosman, D. J.** 2003. Molecular mechanisms of iron uptake in fungi. Mol. Microbiol. **47:**1185–1197.
21. **Kramer, C., G. Kreisel, K. Fahr, J. Kassbohrer, and D. Schlosser.** 2003. Degradation of 2-fluorophenol by the brown-rot fungus *Gloeophyllum striatum*: evidence for the involvement of extracellular Fenton chemistry. Appl. Microbiol. Biotechnol. **64:**387–395.
22. **Kuan, I. C., and M. Tien.** 1993. Stimulation of Mn-peroxidase activity: a possible role for oxalate in lignin biodegradation. Proc. Natl. Acad. Sci. USA **90:**1242–1246.
23. **Martínez, A. T., M. Speranza, F. J. Ruiz-Duenas, P. Ferreira, S. Camarero, F. Guillén, M. J. Martínez, A. Gutiérrez, and J. C. del Río.** 2005. Biodegradation of lignocellulosics: microbial, chemical, and enzymatic aspects of the fungal attack of lignin. Int. Microbiol. **8:**195–204.
24. **Martínez, M. J., F. J. Ruiz-Dueñas, F. Guillén, and A. T. Martínez.** 1996. Purification and catalytic properties of two manganese-peroxidase isoenzymes from *Pleurotus eryngii*. Eur. J. Biochem. **237:**424–432.
25. **Muheim, A., R. Waldner, D. Sanglard, J. Reiser, H. E. Schoemaker, and M. S. A. Leisola.** 1991. Purification and properties of an aryl-alcohol dehydrogenase from the white-rot fungus *Phanerochaete chrysosporium*. Eur. J. Biochem. **195:**369–375.
26. **Muñoz, C., F. Guillén, A. T. Martínez, and M. J. Martínez.** 1997. Laccase isoenzymes of *Pleurotus eryngii*: characterization, catalytic properties and participation in activation of molecular oxygen and Mn^{2+} oxidation. Appl. Environ. Microbiol. **63:**2166–2174.
27. **Muñoz, C., F. Guillén, A. T. Martínez, and M. J. Martínez.** 1997. Induction and characterization of laccase in the ligninolytic fungus *Pleurotus eryngii*. Curr. Microbiol. **34:**1–5.
28. **Park, J. S. B., P. M. Wood, M. J. Davies, B. C. Gilbert, and A. C. Whitwood.** 1997. A kinetic and ESR investigation of iron(II) oxalate oxidation by hydrogen peroxide and dioxygen as a source of hydroxyl radicals. Free Radic. Res. **27:**447–458.
29. **Pera-Titus, M., V. García-Molina, M. A. Baños, J. Giménez, and S. Esplugas.** 2004. Degradation of chlorophenols by means of advanced oxidation processes: a general review. Appl. Catal. B **47:**219–256.
30. **Pignatello, J. J., E. Oliveros, and A. MacKay.** 2006. Advanced oxidation processes for organic contaminant destruction based on the Fenton reaction and related chemistry. Crit. Rev. Environ. Sci. Technol. **36:**1–84.
31. **Popp, J. L., B. Kalyanaraman, and T. K. Kirk.** 1990. Lignin peroxidase

oxidation of Mn^{2+} in the presence of veratryl alcohol, malonic or oxalic acid, and oxygen. Biochemistry **29:**10475–10480.

32. **Rieble, S., D. K. Joshi, and M. H. Gold.** 1994. Purification and characterization of a 1,2,4-trihydroxybenzene 1,2-dioxygenase from the basidiomycete *Phanerochaete chrysosporium*. J. Bacteriol. **176:**4838–4844.

33. **Saparrat, M. C. N., F. Guillén, A. M. Arambarri, A. T. Martínez, and M. J. Martínez.** 2002. Induction, isolation, and characterization of two laccases from the white-rot basidiomycete *Coriolopsis rigida*. Appl. Environ. Microbiol. **68:**1534–1540.

34. **Schoemaker, H. E.** 1990. On the chemistry of lignin degradation. Recl. Trav. Chim. Pays-Bas **109:**255–272.

35. **Schoemaker, H. E., E. M. Meijer, M. S. A. Leisola, S. D. Haemmerli, R. Waldner, D. Sanglard, and H. W. H. Schmidt.** 1989. Oxidation and reduction in lignin biodegradation, p. 454–471. *In* N. G. Lewis and M. G. Paice (ed.), Plant cell wall polymers: biogenesis and biodegradation. ACS Symposium Series 399. American Chemical Society, Washington, DC.

36. **Schoemaker, H. E., U. Tuor, A. Muheim, H. W. H. Schmidt, and M. S. A. Leisola.** 1991. White-rot degradation of lignin and xenobiotics, p. 157–174. *In* W. B. Betts (ed.), Biodegradation: natural and synthetic materials. Springer-Verlag, London, United Kingdom.

37. **Skoumal, M., P. L. Cabot, F. Centellas, C. Arias, R. M. Rodriguez, J. A. Garrido, and E. Brillas.** 2006. Mineralization of paracetamol by ozonation catalyzed with Fe^{2+}, Cu^{2+} and UVA light. Appl. Catal. B **66:**228–240.

38. **Somogyi, M.** 1945. A new reagent for the determination of sugars. J. Biol. Chem. **160:**61–73.

39. **Stahl, J. D., and S. D. Aust.** 1995. Properties of a transplasma membrane redox system of *Phanerochaete chrysosporium*. Arch. Biochem. Biophys. **320:**369–374.

40. **Suzuki, M. R., C. G. Hunt, C. J. Houtman, Z. D. Dalebroux, and K. E. Hammel.** 2006. Fungal hydroquinones contribute to brown rot of wood. Environ. Microbiol. **8:**2214–2223.

41. **Varela, E., and M. Tien.** 2003. Effect of pH and oxalate on hydroquinone-derived hydroxyl radical formation during brown rot wood degradation. Appl. Environ. Microbiol. **69:**6025–6031.

42. **Vinodgopal, K., and J. Peller.** 2003. Hydroxyl radical-mediated advanced oxidation processes for textile dyes: a comparison of the radiolytic and sonolytic degradation of the monoazo dye Acid Orange 7. Res. Chem. Intermed. **29:**307–316.

43. **Vinodgopal, K., J. Peller, O. Makogon, and P. V. Kamat.** 1998. Ultrasonic mineralization of a reactive textile azo dye, Remazol black B. Water Res. **32:**3646–3650.

44. **Vogelpohl, A., and S. M. Kim.** 2004. Advanced oxidation processes (AOPs) in wastewater treatment. J. Ind. Eng. Chem. **10:**33–40.

45. **Zapanta, L. S., and M. Tien.** 1997. The roles of veratryl alcohol and oxalate in fungal lignin degradation. J. Biotechnol. **53:**93–102.